Segmented waveguide tapers for low insertion loss, high performance *SPE:LiNbO$_3$* integrated circuits

Davide Castaldini (1-2-3), Paolo Bassi (1-3), Guillaume Bertocchi (2),
Sorin Tascu (2), Pierre Aschieri (2), Marc De Micheli (2), Sebastien Tanzilli (2) and Pascal Baldi (2)
1) Dipartimento di Elettronica Informatica e Sistemistica, University of Bologna, Italy (e-mail: dcastaldini@deis.unibo.it)
2) Laboratoire de Physique de la Matière Condensée, University of Nice - Sophia Antipolis, France
3) also with MIST.E-R, Laboratory for MIcro and Submicro enabling Technologies of Emilia-Romagna

Abstract: *We present the results of an experimental study of waveguide tapers realized with segmented waveguides in $LiNbO_3$ substrates using the Soft Proton Exchange (SPE) technique. Measurements show that the tapers can be favorably introduced between the nonlinear or electro-optic part of the components, which requires strong mode confinement to increase efficiency, and the coupling section with a standard optical fiber, which requires low mode confinement, in order to have low coupling losses. These tapers allow almost lossless mode shape transformation with a reduction of the coupling losses up to* 0.7 *dB, thus proving the practical interest of the approach. As an example, the use of such tapers in a real integrated optical circuit is shown.*

Introduction

Insertion losses have always been a major problem in Integrated Optics (IO). Reducing the insertion losses is important for telecom and sensors applications and is mandatory in the case of Quantum Communication, where the information is carried by single photons and where amplifiers are not allowed. Losses are due to misalignments, Fresnel reflection and mode mismatch. Misalignments between fiber and IO device can be avoided using careful aligning procedures. Fresnel reflection losses, due to the different values of the refractive indices of the IO waveguide and the optical fiber, can be reduced using index matching fluids or antireflection coatings at the end-face of the sample. Mode mismatch losses are due to different mode sizes in the IO waveguide and the fiber. They are particularly important in the case of active electro-optic (EO) or nonlinear (NL) devices where the component efficiency is a growing function of the mode confinement. In these cases, designing the waveguide to optimize its coupling with low confinement telecom single mode fibers is far from being optimum, but is the more commonly used technique [1] since we are still missing a practical and cost effective solution allowing longitudinal variation of the transversal section of the waveguide mode. This mode size transformer (taper) should be adiabatic, as short as possible, in order to realize the best trade off between propagation losses and coupling efficiency. In the literature a lot of solutions for the design of a taper has been proposed [2, 3, 4, 5]. Among them, the segmented waveguide configuration seems the most suitable as it does not introduce additional steps in the fabrication process [6, 7, 8, 9, 10, 11].

In principle, this technique is rather general, and can be adapted to any material or waveguide fabrication technique. Nevertheless, as the excess losses induced by the segmentation depend very much on material and waveguide fabrication technique, each case has to be carefully studied experimentally. In this paper, we present a study devoted to waveguides realized in *Z-cut* wafers of $LiNbO_3$ that are commonly used for their good nonlinear properties, allowing for example the fabrication of efficient optical frequency converters and photon pair sources required for quantum communication at telecom wavelengths [12].
In order to realize optical waveguides in this substrate, various techniques have been proposed in the past: outdiffusion [13], titanium diffusion [14], ion implantation [15], proton exchange [16] and its different implementations (simple Proton Exchange [16], Annealed Proton Exchange, APE [17], Soft Proton Exchange, SPE [18]). Among the PE techniques, we choose the SPE process which does not perturb the crystalline structure of $LiNbO_3$ while other ones do [19, 20]. In particular, the ferroelectric domain inversion of PPLN devices used for photon pair generation remains intact after SPE [21]. The reported results show that when pushing the SPE parameters to obtain waveguides with the maximum Δn which allows maximum field confinement, tapers showing an overall reduction of the insertion losses with respect to the untapered waveguide can be successfully realized.
The paper is organized as follows. In the next section, the waveguide taper design and fabrication processes are described. In third section, the different characterization techniques used to evaluate the improvements of the taper are illustrated. In the fourth section, the experimental results obtained with different fabrication parameters of the taper are presented. In the fifth section, the use of the tapers in a real integrated circuit is shown and finally, conclusions are drawn.

Device fabrication

The tested devices are constituted by a taper that transforms the highly confined mode of a continuous waveguide (CWG) to a weakly confined one supported by a segmented waveguide (SWG) as shown in figure 1. To understand the features of the mode of such a waveguide, one should remind that, for wavelengths far away from the band gap, the SWG behavior can be described using the so called equivalent waveguide theorem for periodic structures [22, 23], which says

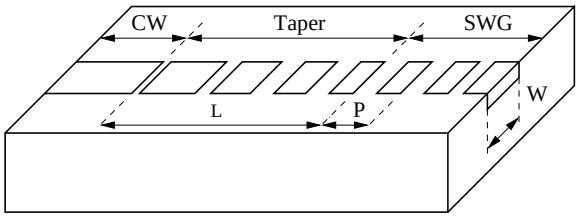

Fig. 1: Schematic of segmented waveguide taper.

that, in this case, a SWG is equivalent to a CWG with the same depth and width but with a surface index equal to:

$$n_{eq} = n_{sub} + \Delta n \cdot DC \tag{1}$$

where n_{sub} is the substrate index, Δn is the step index and DC is the duty cycle defined as the ratio between the length of the high index segment and the period. In the case of a taper, the DC varies from $DC = 1$ (continuous waveguide) to a smaller DC with constant period P so that the surface index of the equivalent waveguide is reduced as well as the mode confinement. Once the desired mode size is reached, the DC is kept constant down to the end of the sample to stabilize the mode size after the transformation in the taper.
Designing the taper one should fix its length (L), the segmentation period (P), the final duty cycle (DC) and the waveguide width (W). Tapers with 48 possible combinations of these parameters (listed in table 1) were first fabricated in order to find the best solution to adopt in the relay.

Table 1: Parameters used for the tapers present on the sample.

$P[\mu m]$	DC	$W[\mu m]$	$L[\mu m]$
15	0.5	5	100
25	0.6	7	600
	0.7		1000
			1400

In order to realize the optical waveguides in the *Z-cut* Lithium Niobate substrate, we have chosen the SPE process. The proton source used is the Benzoic acid with 2.8% of Lithium Benzoate, as this value has been previously shown to give the largest surface extraordinary index variation ($\Delta n = 0.03$ at $\lambda = 632.8nm$) while preserving the original nonlinear optical properties of Lithium Niobate.
The last fabrication step is the end-face polishing to allow end-fire coupling of the sample with the input and output fibers. A particular care is devoted to control the angle between the end-face and the waveguides. Such angle must be 90° in order to use the Fabry-Perot technique to measure the propagation losses [24].

Experimental setup
In this section we describe the experimental setup used to make all the characterizations. The laser source is a tunable external cavity laser emitting between 1.5 μm and 1.6 μm (NetTest Tunics Plus) with an automatic power control system and a narrow linewidth of 150 kHz. In order to control the field polarization state at the entrance of the sample, a monomode polarization maintaining (PM) fiber has been used to couple the source and the waveguides. A standard SMF-28 has then been used to collect the light at the output of the sample. An InGaAs detector allows measuring the light power. The input and output fibers are mounted on piezoelectric translation stages with 16 nm spatial resolution. All the setup is computer controlled via a GPIB interface. This system can be used not only to evaluate separately the IO waveguide propagation losses and the mode overlap integral but also their combined effect, comparing the overall coupling efficiencies using tapered and untapered structures.
The propagation losses are measured using the Fabry-Perot cavity technique [24]. Measuring the power transmitted through the system at different wavelengths, one obtains fringes whose contrast is directly related to the propagation losses. One of the most important advantages of this technique is that the measurement is independent of the coupling efficiency.
The mode mismatch losses can be evaluated via the measurement of the cross-correlation function between waveguide and fiber mode. Such a function is measured by exciting the waveguide under test with a constant power at a fixed wavelength and recording the power collected by the output fiber, while it scans, with 16 nm steps, a 25 $\mu m \times 25$ μm window centered on the waveguide output. Such measurement is similar to that described in [25] and provides many information. First of all we can quantify the tolerance of the fiber to waveguide alignment. A sharp cross-correlation function corresponds to high coupling losses for small alignment errors, while a smooth cross correlation function allows some alignment errors without dramatic impact on the coupling losses. Moreover, knowing the cross-correlation function and the fundamental mode pattern Ψ_f of the SFM-28 fiber, it is possible to reconstruct the waveguide mode field distribution Ψ_w through a simple deconvolution operation. The intensity overlap integral holds then:

$$I = \frac{\left|\iint \Psi_{SWG} \cdot \Psi_f^* dS\right|^2}{\iint |\Psi_{SWG}|^2 \, dS \cdot \iint \left|\Psi_f\right|^2 dS}. \tag{2}$$

Evaluating this integral for different tapers allows determining the combination of parameters which gives the better mode matching.
Finally, the overall coupling efficiency improvement, which depends on the combined effect of taper induced propagation losses and waveguide to fiber mode matching improvement can be evaluated comparing the maximum power transmitted through the different waveguides present on the sample under test. For each waveguide, the throughput power is measured optimiz-

ing contemporarily the positions of both input and output fibers with piezo-controlled stages.

Taper characterization

We have first characterized the sample with structures made by continuous waveguides and tapers in correspondence at one end-face. Figure 2 presents the mode size as a function of the *DC* of the SWG for $W = 5\ \mu m$ and a period $P = 15\ \mu m$. Note that for $DC = 1$, corresponding to a continuous waveguide, we found mode sizes smaller than the fiber mode size (dashed line). Reducing the *DC* the SWG mode size increases as expected. It is then possible to calculate the overlap integral between the fiber and the waveguide modes using the expression 2. The result is reported in figure 3. For

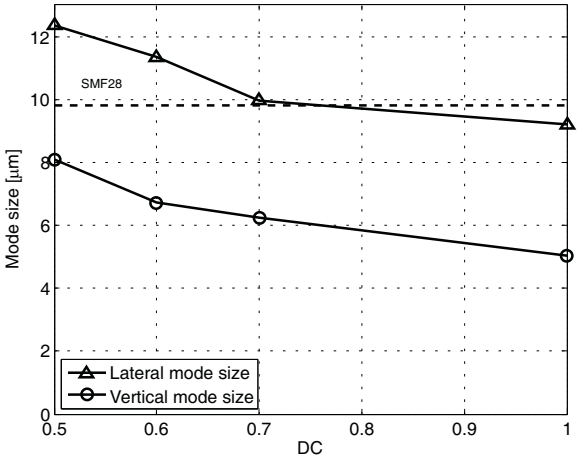

Fig. 2: Measurement of the lateral and vertical mode sizes (at $1/e$ of the field maximum) of SWGs as a function of *DC* with $W = 5\ \mu m$ and $P = 15\ \mu m$.

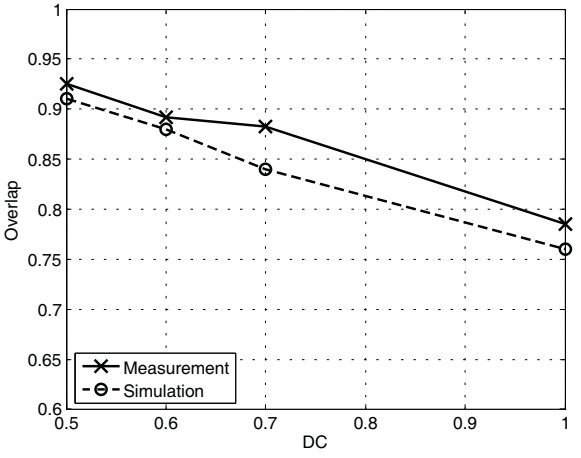

Fig. 3: Overlap between the segmented waveguide mode and the SMF-28 mode for different DC. Measurements (continuous line with crosses) are compared to simulation results (dashed line with circles).

the continuous waveguide we found that the overlap is 78% but the use of a segmented waveguide taper can improve it up to 92% for $DC = 0.5$ (continuous line). This corresponds to an improvement of 0.71 *dB* in logarithmic scale. This experimental result agrees with the numerical prediction obtained using a 3D BPM [26] (dashed line in figure 3). However, this result is not the real performance improvement, which can be obtained using tapered and segmented waveguides, as they induce extra propagation losses which are not taken into account in the overlap integral. These extra propagation losses are due to imperfect mode transformation and scattering losses at the segments edges. So, the use of a segmented waveguide taper becomes effective if the mode matching improvement is larger than the propagation loss increase. Using the Fabry-Perot cavity technique, illustrated in the previous section, we obtained the best result with a 1400 μm long taper associated to a 2600 μm long segmented waveguide, with $P = 15\ \mu m$, $W = 5\ \mu m$ and $DC = 0.5$. In this case we found a loss increase of only 0.04 *dB* with respect to the continuous waveguide. The total improvement obtained in terms of waveguide to fiber coupling is then $0.71 - 0.04 = 0.67\ dB$. The precision of this result is estimated to be around $\pm 0.2\ dB$.

The overall improvement was also measured evaluating the insertion losses difference between a tapered and an untapered waveguide. The results are reported in the table 2 where P_t and P_{CWG} are output powers measured at the end of the waveguides with and without taper respectively. Negative results correspond to the cases where the overlap improvement does not even compensate for the additional losses. The optimum length of the taper depends on the segmentation parameters. Table 2 reports the results for the lengths that provide the best performances.

Table 2: Insertion losses difference between tapered and an untapered waveguides for the different fabrication parameters.

$W[\mu m]$	$P[\mu m]$	$L[\mu m]$	DC	$10\log(P_t/P_{CWG})$ $[dB]$
5	15	1400	0.5	0.78
		1000	0.6	0.22
		600	0.7	0.19
	25	1400	0.5	-0.53
		1400	0.6	0.15
		600	0.7	0.51
7	15	1400	0.5	0.06
		1000	0.6	-0.25
		600	0.7	0.20
	25	1400	0.5	0.37
		1400	0.6	0.43
		600	0.7	0.47

In the case of the best result previously considered, we obtained an overall increase of 0.78 *dB* of the transmitted power with respect to the continuous waveguide. The precision of this measurement is around $\pm 0.1\ dB$. These two different measurements give re-

sults, which taking into account the uncertainties, are equal and confirm the practical interest of segmented waveguide tapers realized using the SPE process.

Integrated optical circuit with tapers

As an example of such practical interest, we now show the use of similar tapers in an integrated optical circuit specially developped for the realization of a quantum relay. The aim of such a device is to increase the achievable distance of quantum communications between two partners [27]. The scheme of the integrated realized device we tested is shown in figure 4.

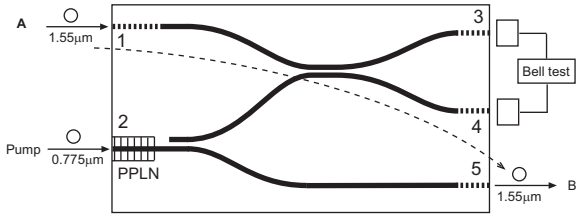

Fig. 4: Schematic of the quantum relay with tapers (dashed lines) at ports 1, 3, 4 and 5.

The performances of such an integrated quantum relay are extremely penalized by coupling losses as four of the five port interact with standard telecommunication fibers (ports 1, 3, 4, 5) at 1.55 μm. The presence of tapers to improve coupling efficiency is then of great interest.

In order to evaluate the insertion losses reduction induced by segmented waveguide tapers in quantum relay we have fabricated tapered and untapered structures on the same sample. The taper parameters correspond to the best result obtained with the previous study. The relay characterization consists of injecting a constant power in port 1 using a PM fiber and to measure the output powers P3 and P4 at port 3 & 4 using two SMF-28 fibers and a powermeter. The total output power (P3+P4) measured for relays that include tapers is 1.28 ± 0.5 dB higher than that obtained with bared ones. This means that each taper induces a coupling losses reduction of 0.64 ± 0.25 dB which is in agreement with the previously described results obtained for straight waveguides.

Conclusion

In this work we have presented experimental results concerning segmented waveguide tapers fabricated in $LiNbO_3$ by the SPE process. Such tapers have also been successfully introduced in an integrated optical circuit developed to realize an integrated optical quantum relay. We have found that, for each interconnection, the introduction of optimized tapers allows reducing by 0.64 dB the coupling losses between the relay and a standard SMF-28 fiber. This result will allow improving the performances of the relay and any other insertion-loss sensitive device.

Acknowledgments

Davide Castaldini gratefully acknowledges Università Italo Francese (http://www.universita-italo-francese.org) for providing him the PhD Vinci fellowship which allowed his participation to this project. This work was supported in part by the U.S. Department of Commerce under Grant BS123456, the Italian Ministry of Education, University and Research (MIUR) and Regione Emilia Romagna in the framework of the *MIST.E-R* Project.

References

[1] R. C. Alferness et al, IEEE J. Quant. Elect., vol. 18, p. 1807, 1982

[2] P. G. Suchoski et al, IEEE J. Lightwave Technol., vol. 5, p. 1246, 1987

[3] K. Kasaya et al, IEEE Photonics Tech. Lett., vol. 5, p. 345, 1993

[4] B. Luyssaert et al, IEEE J. Lightwave Technol., vol. 23, p. 2462, 2005

[5] F. Van Laere et al, ECOC, Paper Tu1.4.5, 2006

[6] M. H. Chou et al, Opt. Lett., vol. 21, p. 794, 1996

[7] F. Dorgeuille et al, Opt. Lett., vol. 20, p. 581, 1995

[8] M. M. Spuhler et al, IEEE J. Lightwave Technol., vol. 16, p. 1680, 1998

[9] Z. Weissman et al, Electr. lett., vol. 28, p. 1514, 1992

[10] Z. Weissman et al, IEEE J. Lightwave Technol., vol. 13, p. 2053, 1995

[11] M. Yanagisawa et al, IEEE Photonics Tech. Lett., vol. 4, p. 433, 1993

[12] O. Alibart et al, Opt. Lett., vol. 30, p. 1539, 2005

[13] J. R. Carruthers et al, App. Opt., vol. 13, p. 2333, 1974

[14] G. J. Griffiths et al, IEEE J. Quant. Elect., vol. 20, p. 149, 1984

[15] M. L. Shah, App. Phys. Lett, vol. 26, p. 652, 1975

[16] J. L. Jackel et al, App. Phys. Lett, vol. 41, p. 607, 1982

[17] M. L. Bortz et al, Opt. Lett., vol. 16, p. 1844, 1991

[18] L. Chanvillard et al, Appl. Phys. Lett., vol. 76, p. 1089, 2000

[19] Yu. N. Korkishko et al, IEEE J. Sel. Topics in Quant. Electr., vol. 2, p. 187, 1996

[20] C. Canali et al, J. Appl. Phys, vol. 59, p. 2643, 1986

[21] Yu. N. Korkishko et al, JOSA A, vol. 18, p. 1186, 2001

[22] Z. Weissman et al, IEEE J. Lightwave Technol., vol. 11, p. 1831, 1993

[23] P. Aschieri et al, App. Opt., vol. 38, p. 5734, 1999

[24] R. Regener et al, Appl. Phys B, vol. 36, p. 143, 1985

[25] D. Hannappe et al, Appl. Opt., vol. 35, p. 659, 1996

[26] F. Fogli et al, IEEE J. Lightwave Technol., vol. 17, p. 136, 1999

[27] D. Collins et al, J. Mod. Opt., vol. 52, p. 735, 2005